# Calcium Binding Properties of an Epidermal Growth Factor-like Domain from Human Thrombomodulin†

Dmitri Tolkatchev‡ and Feng Ni*,§

*Department of Biochemistry, McGill University, Montreal, Quebec, Canada H3G 1Y6, and Biomolecular NMR Laboratory and the Montreal Joint Centre for Structural Biology, Biotechnology Research Institute, National Research Council of Canada, 6100 Royalmount Avenue, Montreal, Quebec, Canada H4P 2R2*

*Received December 9, 1997; Revised Manuscript Received March 26, 1998*

ABSTRACT: Two different disulfide-paired isomers of the peptide $T_{422}$DIDECENG$_{430}$GFCSGVCHNL$_{440}$-PGTFECISG$_{449}$, spanning the junction between the fifth and sixth EGF-like domains plus the N-terminal part of the sixth EGF-like domain from human thrombomodulin (TM), and containing a consensus calcium binding sequence, were synthesized and studied by two-dimensional proton NMR spectroscopy. In the course of air oxidation of the fully reduced form of the peptide, only uncrossed non EGF-like [1−2, 3−4] disulfide-bonded isomer was produced, regardless of the presence of redox buffer and/or calcium. The crossed [1−3, 2−4] isomer was prepared from a peptide with acetamidomethyl-protected second and fourth cysteines. The isomer with the crossed disulfide pairing was a better thrombin inhibitor and was more strongly affected by calcium binding than the uncrossed [1−2, 3−4] isomer. Calcium-induced NMR resonance shifts observed for the [1−3, 2−4] isomer provide evidence for the presence of a specific calcium-binding site in the corresponding TM region. There was a limited dispersion of the proton chemical shifts and a general lack of nonsequential NOE's for both peptide isomers in the presence or absence of calcium. Therefore, neither the apo nor the calcium-bound forms of the peptides adopted a completely folded conformation, despite the fact that the [1−3, 2−4] isomer contains a potential folding nucleus existing in a number of disulfide-rich proteins. Apparently, other interactions have to be involved to determine the three-dimensional structure of the criss-cross fold in this peptide, most likely the interaction with the C-terminal parts of the fifth and/or sixth EGF-like domains.

Thrombomodulin (TM)[1] is an endothelial cell membrane glycoprotein which alters the functions of thrombin (IIa). The formation of a 1:1 IIa−TM complex leads to the decrease of thrombin's activity toward fibrinogen and a marked increase of thrombin's activity toward protein C (*1*). Activated with the IIa−TM complex, protein C, in turn, shuts down the production of thrombin by cleaving and inactivating factors Va and VIIIa (*2*, *3*). Thus, TM directly inhibits the coagulant activity of thrombin and turns thrombin into an anticoagulant.

The region responsible for the cofactor activity of TM is located within its epidermal growth factor (EGF) homology domains and is comprised of the last three (fourth, fifth, and sixth) EGF-like domains (EGF456 fragment) (*4*, *5*). Each EGF-like repeat contains six cysteines which presumably form three disulfide bonds analogous to those found in EGF itself (*6*) and in some other EGF-like domains (*7*−*10*). The modular nature of the EGF-like domains in TM has been demonstrated by the structural studies of TM fragments. Up to date the structures of the fourth and fifth EGF-like domains from TM and their fragments (*7*, *11*−*13*) have been established.

Almost all known 3D structures of EGF-like domains from different sources resemble that of EGF and are consistent with the EGF [1−3, 2−4, 5−6] disulfide pairing pattern (*7*, *14*−*23*). Most of the fragments are quite similar to the EGF molecule and they have an N-terminal two-stranded antiparallel $\beta$-sheet cemented by the 1−3 and 2−4 cystines, followed by a short C-terminal double hairpin cemented by the 5−6 cystine (*14*−*22*). The C terminal [5−6] loops of the second EGF-like repeat from factor X (*23*) and the fourth EGF-like repeat from TM (*7*) have four and five amino acid insertion, respectively, and they have a broadened shape that does not superimpose well on the corresponding EGF loop.

Since the S−S linked EGF-like modules in free and IIa-bound EGF456 fragment are expected to have a more or less conserved structure, it is important to visualize structural features of the bridging peptides between the fourth, fifth, and sixth EGF-like repeats defining the mutual orientation of the EGF-like modules. In addition to inter-EGF−domain interactions and TM−IIa interactions, calcium binding may markedly affect the conformation of EGF456. Nagashima

† The work was supported in part by a grant from the Medical Research Council of Canada (MT-12566) and by the National Research Council of Canada (NRCC publication No. 41428).

* Author to whom correspondence should be addressed.

‡ McGill University.

§ National Research Council of Canada.

[1] Abbreviations: EGF, epidermal growth factor; IIa, thrombin; TM, thrombomodulin; EGF456, a fragment of thrombomodulin consisting of the fourth, fifth, and sixth epidermal growth factor-like domains; EGF56, a fragment of thrombomodulin consisting of the fifth and sixth epidermal growth factor-like domains; TCEP, tris-(2-carboxyethyl)-phosphine; DSS, sodium 2,2-dimethyl-2-silapentane-5-sulfonate; Acm, acetamidomethyl; DCT, the concentration of a peptide required to double the clotting time.

S0006-2960(97)03024-9 CCC: $15.00 
Published on Web 06/05/1998

et al. (*24*) noted that the region of TM spanning residues 423−444 and thus comprising the junction between the fifth and sixth EGF-like modules plus the N-terminal part of the sixth EGF-like module, contains a consensus sequence for a calcium-binding site. The sequence, DIDEC-XXXXX-C−XXX-C-X-N-XXXX-F-X-C-X-C, is homologous to known calcium-binding EGF-like domains in factor IX (*25*, *26*), fibrillin-1 (*27*−*29*), protein S (*30*), factor X (*31*), and protein C (*32*). Although the existence of the calcium binding site may be an important structural feature of this IIa-binding region of TM, very little direct data supporting the presence and importance of a calcium-binding site in this region are available so far. It was shown, however (*24*), that alanine substitution of the residues presumably participating in the calcium binding led to a large decrease in TM cofactor activity.

To obtain direct information on calcium binding of EGF56, we synthesized a peptide comprising the junction between the fifth and sixth EGF-like modules plus the N-terminal part of the sixth EGF-like module of TM, $T_{422}$DIDECENG$_{430}$-GFCSGVCHNL$_{440}$PGTFECISG$_{449}$, and studied its interaction with $Ca^{2+}$ in solution by one- and two-dimensional proton ($^1$H) NMR. This fragment also contains a potential folding subdomain within the EGF-like repeat (*33*, *34*) and belongs to an abundant disulfide-reinforced structural scaffold known as T-knot motif (*33*). Although the peptide does not represent the full sixth EGF-like domain we expected it to behave as an independent minimal architectural kernel responsible for calcium binding in TM.

## EXPERIMENTAL PROCEDURES

*Sample Preparation*. The synthetic peptides, $T_{422}$-DIDECENG$_{430}$GFCSGVCHNL$_{440}$PGTFECISG$_{449}$ (28EG56) and $T_{422}$DIDECENG$_{430}$GFC(Acm)SGVCHNL$_{440}$PGTFEC-(Acm)ISG$_{449}$ (28EG56acm), where C(Acm) stands for an acetamidomethyl protected cysteine, were prepared by solid-phase peptide synthesis using standard Fmoc chemistry on an Applied Biosystems 431A peptide synthesizer. Cys448 of the original sequence was replaced by Ser to avoid undesirable disulfide coupling during the regio-selective oxidation of the peptide samples. The synthetic peptides were dissolved in 0.1 M Tris-HCl, 1 mM EDTA, 100 mM DTT, pH 8.3, at a peptide concentration of 5−10 mg/mL, and incubated under argon for several hours. The reduced peptides were purified by HPLC using a $C_{18}$ Vydac column and a linear 10−45% acetonitrile gradient in 0.1% trifluoroacetic acid (TFA), at a flow rate of 2−5 mL/min. One-step free-air oxidation of the peptides was performed overnight in 1% ammonium acetate buffer, pH 8.5, or in 50 mM Tris-HCl buffer, pH 8.5, at a peptide concentration of approximately 6 $\mu$g/mL. After the oxidation was complete the peptides were loaded on a Vydac $C_{18}$ HPLC column and eluted with a linear 10−45% acetonitrile gradient in 0.1% TFA. To perform the second-step oxidation of the Acm-blocked peptide, repurified and lyophilized peptide was dissolved in 0.8 mL of 50% TFA at the concentration of approximately 1 mM. A solution of $I_2$ in methanol (5−10 mM) was added dropwise until the yellowish color remained, and the mixture was stirred for 20 min under argon (*35*). After that the reaction mixture was cooled on ice and the nonreacted $I_2$ was reduced with sodium thiosulfate. The mixture was neutralized with ammonium hydroxide and applied on the Vydac $C_{18}$ HPLC column. When necessary, the oxidatively folded peptides were repurified on a Vydac $C_8$ pH-resistant HPLC column using a linear 10−45% acetonitrile gradient, where solvent A was 1% ammonium bicarbonate, and desalted on Sep-Pak C18 cartridges. SCIEX API *III* ion-spray mass spectrometer was used to confirm that the oxidation reactions were complete.

For NMR measurements the peptides were dissolved in 20 mM sodium acetate-$d_3$ buffer to a final concentration of 0.5−1.0 mM. A volume of 45 $\mu$L of $D_2O$ was added to 400 $\mu$L of the peptide solution to provide the NMR deuterium lock signal. The pH of the samples was adjusted to 5.5 with 100 mM NaOH or HCl. For the binding of metal ions, 1 M $CaCl_2$, 1M $MgCl_2$, or 4 M NaCl was added to the sample in small aliquots in the same 20 mM sodium acetate-$d_3$ buffer, pH 5.5.

*Determination of Disulfide Bonds*. The disulfide-bonding pattern of the isomers was determined by a partial reduction method (36, 37). The reductant tris-(2-carboxyethyl)-phosphine (TCEP) was synthesized from tris-(2-cyanoethyl)-phosphine (Strem) by the method of Burns et al. (*38*). The [1−2, 3−4] isomer was reduced for 4 min and the [1−3, 2−4] isomer was reduced for 12 min in an aqueous solution containing 20 mM TCEP and 0.17 M citric acid, pH 3.0. After that, the mixtures were immediately injected onto HPLC. The resulting partially reduced species were isolated on an analytical Vydac $C_{18}$ HPLC reverse-phase column and alkylated with a supersaturated 2.2 M solution of iodoacetamide as described in (*36*). The alkylated peptides were purified on HPLC and characterized by N-terminal sequencing. Ion-spray mass spectrometry was used to monitor the course of the reactions.

*Clotting Assay*. The clotting assays were performed in 50 mM Tris-Cl, 100 mM NaCl, 0.1% poly(ethylene glycol) 8000, 0.1% bovine plasma fibrinogen (Sigma), pH 7.6, at 37 °C. Each assay mixture contained a certain concentration of the peptide, and the reaction was started by the addition of human thrombin to a final concentration of 0.1 unit/mL. To determine the clotting time the optical absorbance of the assay mixtures was detected at 420 nm.

*NMR Experiments*. One- and two-dimensional NMR experiments were carried out on Bruker AMX2-500 and DRX-500 NMR spectrometers using procedures as described previously (*39*, *40*). TOCSY (*41*, *42*) and flip-back NOESY (*43*) spectra were obtained at 15 and 30 °C without spinning the sample. NOESY experiments were performed with a mixing time of 250 ms. Spectral processing was carried out using FELIX (Hare Research) and an in-house program, nmrdsp, on Silicon Graphics workstations. The Sybyl software package (TRIPOS Inc.) was used for spectral vizualization.

*Proton Resonance Assignments*. Residue-specific assignments of the proton resonances were achieved by spin system identification using TOCSY, followed by sequential assignments through NOE connectivities. Despite the number of residues with similar spin types, the dispersion of the amide proton resonances was sufficiently large to allow the unambiguous assignments of all the proton resonances in the absence and presence of metal ions. All chemical shift values were determined from the two-dimensional spectra and reported with respect to the DSS signal which was set to 0 ppm.

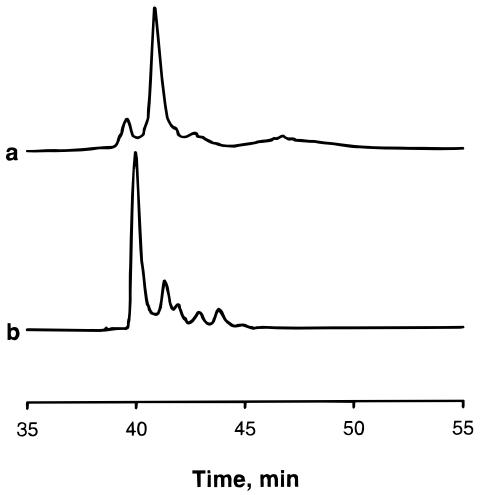


FIGURE 1: HPLC purification of the [1−2, 3−4] (a) and [1−3, 2−4] (b) disulfide-bonded isomers of $T_{422}$DIDECENG$_{430}$-GFCSGVCHNL$_{440}$PGTFECISG$_{449}$. (a) The synthetic peptide 28EG56 was reduced in 0.1 M Tris Cl, 1 mM EDTA, 100 mM DTT, pH 8.3, and purified as described in Experimental Procedures. The fraction corresponding to the reduced species of the desired sequence was collected and added to 1 L of 1% ammonium acetate buffer, pH 8.5. The mixture was stirred overnight at room temperature, and the products of oxidation were loaded onto a 25 × 1.0 cm Vydac $C_{18}$ reverse-phase HPLC column equilibrated with 10% acetonitrile, 0.1% TFA. The separation was performed at a flow rate of 2 mL/min using an extended gradient of 90% solution A (0.1% TFA), 10% solution B (0.1% TFA in acetonitrile) for 10 min, 10−20% solution B over 10 min, 20−45% solution B over 50 min. Zero time corresponds to the moment of sample injection. The major peak with a retention time of 41 min was collected and repurified, and it was shown to have [1−2, 3−4] bonding pattern (see text). (b) The synthetic peptide 28EG56Acm was air-oxidized and purified similarly to 28EG56. The Acm removal and the second-step oxidation of the repurified circlized 28EG56Acm with the help of iodine was performed as described in Experimental Procedures. The neutralized oxidation mixture was loaded onto a 25 × 1.0 cm Vydac $C_{18}$ reverse-phase HPLC column and purified using the same separation conditions as for the [1−2, 3−4] isomer. The major peak with retention time of 40 min was repurified and it was shown to have the expected mass of 2900.

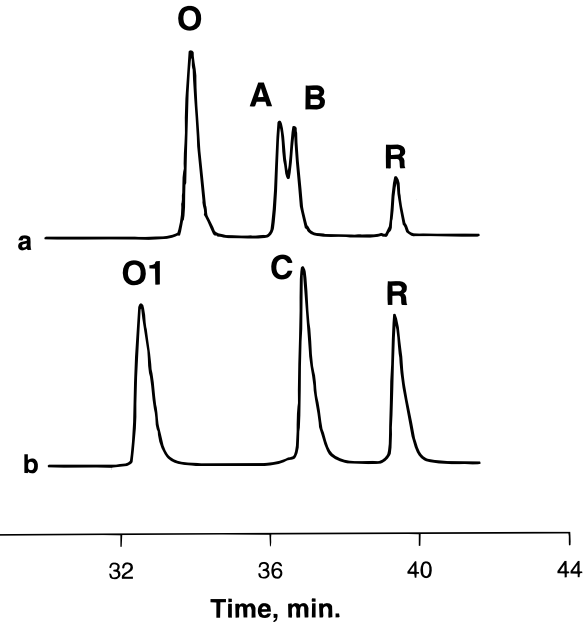


FIGURE 2: HPLC separation of the partially reduced products of the [1−2, 3−4] and [1−3, 2−4] disulfide-bonded isomers. The [1−2, 3−4] (a) and [1−3, 2−4] (b) isomers were partially reduced with TCEP as described in Experimental Procedures and immediately applied to a 25 × 0.46 cm Vydac $C_{18}$ reverse-phase HPLC column equilibrated with 10% acetonitrile, 0.1% TFA. The separation was performed at a flow rate of 1 mL/min. Other separation conditions were as in Figure 1. O and O1 indicate the elution peaks of fully oxidized [1−2, 3−4] and [1−3, 2−4] species, respectively, R, represent completely reduced species of 28EG56, and A, B, and C represent the semireduced species.

## RESULTS

*Disulfide-Bonded Isomers of the 28EG56.* HPLC purification of free-air oxidized peptide 28EG56 gave a single major peak (Figure 1a), with a mass of 2900. The presence of glutathion redox buffer and/or 100 mM $CaCl_2$ in the oxidation mixture did not change the HPLC profile. To establish the disulfide bonding pattern of the free-air oxidized 28EG56, we used the partial reduction technique of Gray (*36*, *37*). The partial TCEP reduction of the oxidized and repurified peptide gave, besides the completely reduced and completely oxidized species, R and O, respectively, two semireduced intermediates, A and B (Figure 2a). These two intermediates were stable in 0.1% TFA for days and no signs of disulfide interexchange were detected. The semi-reduced isomers were alkylated with iodoacetamide (see Experimental Procedures) and repurified. Mass spectrometry showed that upon iodoacetamide treatment two cysteines out of four were alkylated in each isomer, producing species with a mass of 3018. N-terminal amino acid analysis of the first 14 residues for both isomers demonstrated that the first and the second cysteines were labeled for intermediate A, and the third and the fourth for intermediate B. Thus, free-air oxidized 28EG56 has the [1−2, 3−4] disulfide pairing pattern. This pairing differs from the expected EGF-like [1−3, 2−4] pairing and may be a result of removing the fragment from the context of the EGF homology domains of TM.

We forced the formation of the EGF-like [1−3, 2−4] isomer by a two-step oxidation of the Acm-blocked peptide. The peptide with the same primary sequence (28EG56acm) was synthesized with Acm protecting groups on the second and fourth cysteines. At first, 1−3 disulfide bond was formed by free-air oxidation. The formation of the first disulfide bond was confirmed by a decrease of the peak retention time and mass spectrometry. After the resulting cyclized semiproduct was repurified, iodine was used to remove the Acm groups and form the 2−4 disulfide bond (See Experimental Procedures and Figure 1b) producing species with the expected mass of 2900. The [1−3, 2−4] isomer eluted approximately 1 min earlier than the [1−2, 3−4] isomer. To compare with the [1−2, 3−4] isomer, we also performed partial reduction and alkylation of the [1−3, 2−4] isomer. The HPLC analysis of partially TCEP-reduced [1−3, 2−4] isomer showed the completely reduced species, R, the remaining fully oxidized species, O1, and the semireduced species, C (Figure 2b). Peak C contained two semireduced isomers which after alkylation with iodoacetamide were easily resolved by HPLC. The mass spectra of the isomers confirmed labeling of two cysteines in each isomer. N-terminal amino acid analysis of the first 14 residues of one of the alkylated isomer was consistent with the expected forced [1−3, 2−4] pairing.

Since cysteines 2 and 3 are separated with only three residues in the sequence, the formation of [1−4, 2−3]

Table 1: $^1$H Chemical Shifts (ppm from DSS) of (1−2, 3−4) Isomer in 20 mM Sodium Acetate-$d_3$, pH 5.5, at 15 °C

| residue | | HN | αH | βH | γH | δH | other |
|---|---|---|---|---|---|---|---|
| Thr | 1 | | 4.20 | 3.92 | 1.33 | | |
| Asp | 2 | 9.00 | 4.71 | 2.70, 2.55 | | | |
| Ile | 3 | 8.31 | 4.14 | 1.87 | 1.44, 1.19 | 0.83 | |
| Asp | 4 | 8.36 | 4.62 | 2.76, 2.68 | | | |
| Glu | 5 | 8.47 | 4.32 | 2.18, 2.04 | 2.39, 2.39 | | |
| Cys | 6 | 8.54 | 4.45 | 3.17, 3.10 | | | |
| Glu | 7 | 8.57 | 4.18 | 2.06, 2.00 | 2.34, 2.34 | | |
| Asn | 8 | 8.31 | 4.76 | 2.89, 2.75 | | | δNH$_2$ 7.74, 6.99 |
| Gly | 9 | 8.16 | 4.14 | | | | |
| | | | 3.84 | | | | |
| Gly | 10 | 7.99 | 4.06 | | | | |
| | | | 3.81 | | | | |
| Phe | 11 | 8.45 | 4.61 | 3.05, 3.05 | | 7.23, 7.23 | εH 7.32 |
| Cys | 12 | 8.34 | 4.76 | 3.16, 2.97 | | | |
| Ser | 13 | 8.58 | 4.31 | 3.90, 3.90 | | | |
| Gly | 14 | 8.49 | 3.97 | | | | |
| | | | 3.97 | | | | |
| Val | 15 | 7.90 | 4.12 | 2.03 | 0.87, 0.83 | | |
| Cys | 16 | 8.49 | 4.60 | 3.05, 3.05 | | | |
| His | 17 | 8.88 | 4.76 | 3.26, 3.16 | | 7.26 | εH 8.56 |
| Asn | 18 | 8.66 | 4.73 | 2.74, 2.61 | | | δNH$_2$ 7.47, 6.95 |
| Leu | 19 | 8.33 | 4.64 | 1.65, 1.65 | 1.58 | 0.93, 0.93 | |
| Pro | 20 | | 4.32 | 2.31, 1.89 | 2.12, 2.02 | 3.86, 3.64 | |
| Gly | 21 | 8.79 | 4.12 | | | | |
| | | | 3.72 | | | | |
| Thr | 22 | 7.81 | 4.53 | 4.23 | 1.12 | | |
| Phe | 23 | 8.62 | 4.72 | 3.26, 2.93 | | 7.24, 7.24 | εH 7.32 |
| Glu | 24 | 8.22 | 4.32 | 1.95, 1.95 | 2.25, 2.25 | | |
| Cys | 25 | 8.64 | 4.68 | 3.21, 2.95 | | | |
| Ile | 26 | 8.48 | 4.28 | 1.89 | 1.48, 1.20 | 0.85 | γH 0.94 |
| Ser | 27 | 8.56 | 4.50 | 3.88, 3.88 | | | |
| Gly | 28 | 8.09 | 3.79 | | | | |
| | | | 3.79 | | | | |

disulfide bonding isomer in TM appears to be very unlikely, and we did not attempt to prepare and analyze this isomer.

*The Inhibitory Activity of the* [*1−2, 3−4*] *and* [*1−3, 2−4*] *Isomers toward Thrombin*. Both isomers increased the time of fibrinogen clotting catalyzed by IIa. The concentration of the [1−3, 2−4] isomer required to double the clotting time (DCT) was 70 μM, while that of the [1−2, 3−4] isomer was 190 μM. Previously, Longheed et al. (*44*) showed that the cyclic peptide CHNLPGTFEC corresponding to the C3−C4 loop of the [1−2, 3−4] isomer exhibited only weak IIa binding with DCT equal to 0.79 mM. As expected, the longer [1−2, 3−4] isomer had higher binding affinity than its C3−C4 loop. Nevertheless, the isomer with the "correct" [1−3, 2−4] EGF-like disulfide pairing turned out to be a better IIa inhibitor.

*NMR Spectra of the Apo-*[*1−2, 3−4*] *and Apo-*[*1−3, 2−4*] *Isomers*. After oxidation, both isomers were repurified in basic and acidic conditions (see Experimental Procedures). Both peptides showed a unique set of cross-peaks in two-dimensional TOCSY and NOESY NMR spectra. All twenty-eight spin systems of every isomer were accounted for, and the presence of impurities was negligible. The proton chemical shifts from the sequential resonance assignment for the apo forms of the isomers are listed in Tables 1 and 2. The sequential NOE walks for both isomers are shown in Figure 3.

*NMR Analysis of $Ca^{2+}$ Binding*. The addition of 22 mM calcium (as $CaCl_2$) at pH 5.5 caused shifts of some amide, $C^{\alpha}H$, and side chain proton resonances in both [1−2, 3−4] and [1−3, 2−4] isomers (Figure 4). Despite the identical primary sequence of these two peptides, calcium binding affected the [1−3, 2−4] isomer much more strongly than the [1−2, 3−4] isomer. In the same conditions, an increase of up to 100 mM in sodium chloride concentration did not produce detectable changes in the spectra of either of the isomers. Since further increase in NaCl concentration resulted in some spectra changes, we did not study the peptide−calcium interaction at $Ca^{2+}$ concentrations higher than ∼40 mM ($I = 0.08$) to avoid nonspecific ionic strength effects.

For the [1−2, 3−4] isomer, the detectable shifts occurred only within the N-terminal half of the peptide (residues 424−436 of TM). The strongest shifts of the amide protons in the fragment were observed for residues $Asp_{425}$, $Glu_{428}$, and $Gly_{431}$, and for the side chain protons of residues $Glu_{426}$ ($C^{\gamma}H$) and $Asn_{429}$ ($C^{\alpha}H$). Nevertheless, even the strongest shifts were equal to or less than 0.04 ppm (20 Hz) in these conditions. At sodium chloride concentrations higher than 200 mM, the changes caused by the nonspecific ionic strength effects were comparable with the small shifts due to the calcium binding. As a result of rather small spectral changes and the influence from the nonspecific ionic strength effects, it was difficult to obtain a reliable value of the calcium-binding constant for this isomer (Figure 5).

Calcium binding caused much more pronounced changes in the NMR spectra of the [1−3, 2−4] isomer. Upon calcium addition at 15 °C, pH 5.5, the backbone amide proton resonances of many residues were significantly shifted (up to 0.16 ppm) or broadened out. The most affected regions span the residues 425−430 and 438−445 of TM. The amide proton peaks of all three glutamic residues ($Glu_{426}$, $Glu_{428}$, and $Glu_{445}$) and of $His_{438}$ were broadened out and were not

Table 2: $^1$H Chemical Shifts (ppm from DSS) of (1−3, 2−4) Isomer in 20 mM Sodium Acetate-$d_3$, pH 5.5, at 15 °C

| residue | | HN | αH | βH | γH | δH | other |
|---|---|---|---|---|---|---|---|
| Thr | 1 | | 4.19 | 3.91 | 1.32 | | |
| Asp | 2 | 8.99 | 4.68 | 2.75, 2.60 | | | |
| Ile | 3 | 8.30 | 4.10 | 1.82 | 1.43, 1.18 | 0.85 | γH 0.88 |
| Asp | 4 | 8.36 | 4.60 | 2.74, 2.64 | | | |
| Glu | 5 | 8.37 | 4.23 | 2.04, 1.96 | 2.30, 2.30 | | |
| Cys | 6 | 8.50 | 4.51 | 3.01, 2.81 | | | |
| Glu | 7 | 8.37 | 4.23 | 2.04, 1.96 | 2.30, 2.30 | | |
| Asn | 8 | 8.52 | 4.61 | 2.84, 2.75 | | | $\delta NH_2$ 7.65, 6.97 |
| Gly | 9 | 8.32 | 4.01 | | | | |
| | | | 3.81 | | | | |
| Gly | 10 | 8.09 | 3.92 | | | | |
| | | | 3.79 | | | | |
| Phe | 11 | 8.23 | 4.71 | 3.09, 2.95 | | 7.20, 7.20 | εH 7.33, ζH 7.29 |
| Cys | 12 | 8.66 | 4.76 | 3.16, 2.84 | | | |
| Ser | 13 | | 4.46 | 3.96, 3.90 | | | |
| Gly | 14 | 8.33 | 4.02 | | | | |
| | | | 3.93 | | | | |
| Val | 15 | 8.13 | 4.18 | 2.08 | 0.92, 0.87 | | |
| Cys | 16 | 8.34 | 4.59 | 2.68, 2.60 | | | |
| His | 17 | 8.85 | 4.84 | 3.25, 3.12 | | 7.26 | εH 8.55 |
| Asn | 18 | 8.72 | 4.74 | 2.72, 2.72 | | | $\delta NH_2$ 7.54, 7.04 |
| Leu | 19 | 8.26 | 4.67 | 1.57, 1.57 | 1.50 | 0.90, 0.82 | |
| Pro | 20 | | 4.35 | 2.29, 1.93 | 2.12, 2.00 | 3.84, 3.60 | |
| Gly | 21 | 8.76 | 4.10 | | | | |
| | | | 3.78 | | | | |
| Thr | 22 | 7.92 | 4.47 | 4.19 | 1.09 | | |
| Phe | 23 | 8.44 | 4.79 | 3.09, 2.94 | | 7.10, 7.10 | εH 7.25, ζH 7.20 |
| Glu | 24 | 8.47 | 4.45 | 1.96, 1.89 | 2.22, 2.22 | | |
| Cys | 25 | 8.75 | 4.93 | 3.11, 2.96 | | | |
| Ile | 26 | 8.76 | 4.35 | 1.82 | 1.34, 1.08 | 0.76 | γH 0.90 |
| Ser | 27 | 8.64 | 4.52 | 3.87, 3.87 | | | |
| Gly | 28 | 8.11 | 3.78 | | | | |
| | | | 3.78 | | | | |

detectable in TOCSY and NOESY spectra in these conditions. Calcium titration of the position of well-resolved Asn18 $^{\delta}NH_2$ resonances yielded a calcium affinity of 11 mM (Figure 5).

To establish the behavior of the residues with broadened NH resonances at 15 °C (Glu's and His) upon calcium binding, we examined the NMR spectral differences between the calcium-free and calicum-bound [1−3, 2−4] isomer at 30 °C. At the higher temperature, the NH resonance lines sharpened and it was possible to see the cross-peaks from the amide protons of His and Glu's of the calcium-bound peptide in the TOCSY spectra. With the temperature increase, the values of the shifts caused by the addition of calcium were only slightly changed, and the overall pattern of the calcium influence on the isomer remained the same. At 30 °C, the NH shifts of $Glu_{426}$, $Glu_{428}$, $Glu_{445}$, and $His_{438}$ caused by calcium binding were 0.17, 0.12, 0.11, and 0.11 ppm, respectively.

The residues with NH resonance shifts larger than 0.08 ppm ($Asp_{425}$, $Glu_{426}$, $Glu_{428}$, $His_{438}$, $Asn_{439}$, $Leu_{440}$, $Gly_{442}$, $Thr_{443}$, $Glu_{445}$, and $Phe_{444}$) form a region which was presumed to participate in calcium binding (*24*, *25*). Nagashima et al. (*24*) showed that alanine substitution of $Asp_{423}$, $Ile_{424}$, $Asp_{425}$, $Glu_{426}$, $Asn_{429}$, $Asn_{439}$, $Leu_{440}$, and $Phe_{444}$ led to large decreases of TM cofactor activity.

The major calcium-induced changes of the side chain proton resonances occurred within the residues $Asp_{423}$, $Glu_{426}$, $Asn_{439}$, $Leu_{440}$, and $Phe_{444}$. The $C^{\beta}H$ of $Asp_{423}$ and $C^{\gamma}H$ of $Glu_{426}$ resonances were shifted upfield by 0.06 ppm, and the low-field $N^{\delta}H$ resonance of $Asn_{439}$ was shifted downfield by 0.11 ppm. The calcium-induced chemical shift changes for $C^{\beta}H$ of $Leu_{440}$ and $C^{\beta}H$ of $Phe_{444}$ were −0.08 and 0.10 ppm, correspondingly. We believe that the side chains of these residues are likely to be involved in specific interactions caused by calcium binding.

*$Mg^{2+}$ Binding of the [1−3, 2−4] Isomer*. To confirm the specificity of $Ca^{2+}$ binding by the [1−3, 2−4] isomer, we studied the shifts of the peptide resonances caused by the addition of $MgCl_2$. Very little changes were observed in 2D NMR spectra in the presence of 22 mM magnesium, and these changes were less than 0.04 ppm for the NH resonances of $Glu_{426}$, $Glu_{428}$, and $Glu_{445}$, which were the most affected by the magnesium addition. Figures 5 and 6 illustrate the comparative changes of the isomer spectra upon addition of magnesium and calcium.

*Conformations of the [1−2, 3−4] and [1−3, 2−4] Isomers in Solution*. The NH resonances for both isomers in the presence or absence of calcium were poorly dispersed, less than 1.2 ppm (Figure 3) for all cases. Also, only a very few medium- and long-range NOE cross-peaks in both the apo and calcium-bound forms of the isomers were detected. This suggests that the isomers, either calcium-bound or free, are conformationally flexible in solution.

Since the difference between the actual and random-coil values for a $C^{\alpha}H$ resonance is strongly related to the residue conformation (*45*), it was possible to evaluate the potential conformational changes in the [1−3, 2−4] isomer upon calcium binding. Despite the fact that many NH resonances were dramatically changed, particularly for the residues close to the calcium coordination sphere, only a few $C^{\alpha}H$ resonances were shifted in the peptide−calcium complex

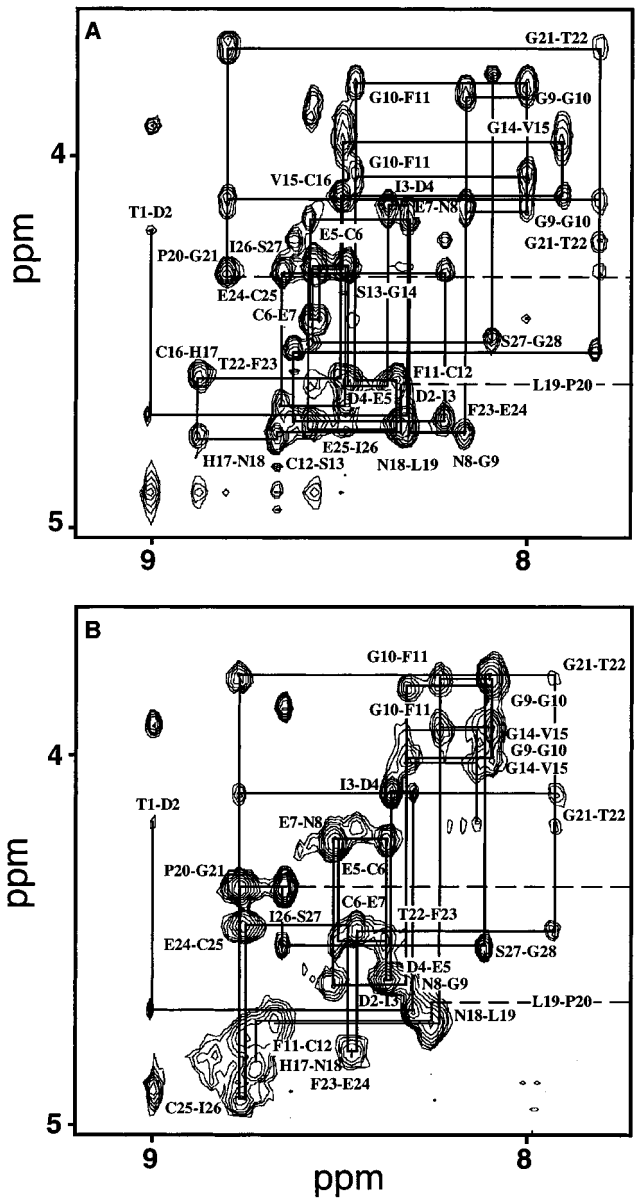


FIGURE 3: Sequential NOE walk for the [1−2, 3−4] and [1−3, 2−4] disulfide-bonded isomers. The [1−2, 3−4] (A) and [1−3, 2−4] (B) isomers were dissolved in 20 mM sodium acetate-$d_3$ buffer, 10% $D_2O$, pH 5.5, and NOESY spectra were acquired at 15 °C. The peaks were assigned by spin system identification using TOCSY, followed by sequential assignments through NOE connectivities.

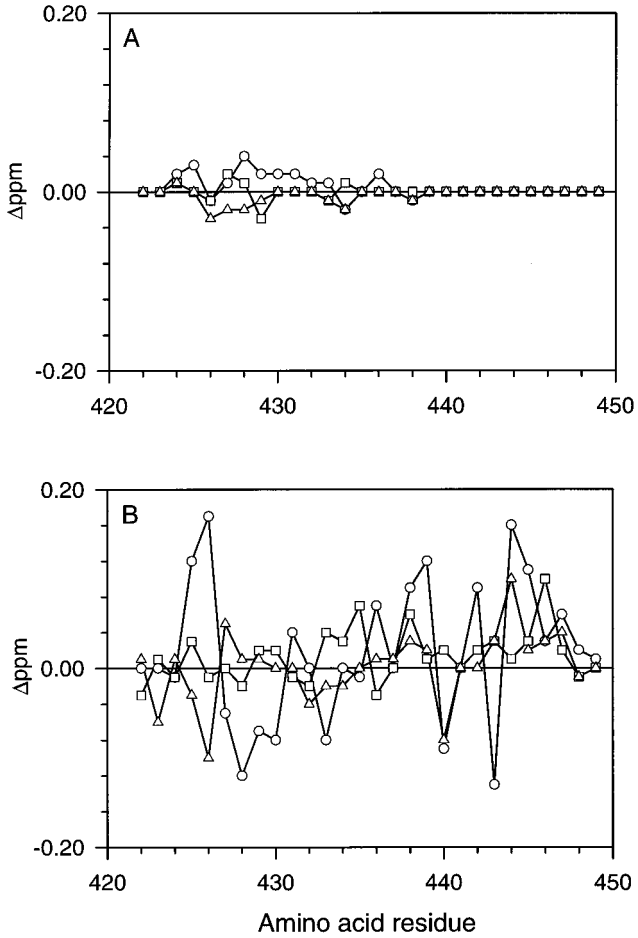


FIGURE 4: Calcium-induced chemical shift changes in [1−2, 3−4] and [1−3, 2−4] disulfide-bonded isomers of 28EG56. The chemical shift changes (○, NH; □, $C^{\alpha}H$; Δ, side-chain protons) caused by the addition of 22 mM $CaCl_2$ to the solution of [1−2, 3−4] (A) and [1−3, 2−4] (B) isomers in 20 mM sodium acetate-$d_3$, 10% $D_2O$, pH 5.5, at 15 °C. The values of NH shift changes for the $Glu_{426}$, $Glu_{428}$, $Glu_{445}$ and $His_{438}$ residues in crossed [1−3, 2−4] isomer were taken from the data obtained at 30 °C. Other NH shifts were insignificantly changed with the temperature increase.

(Figures 4 and 7). $Asp_{425}$, $Val_{436}$, $Thr_{443}$, and $Glu_{445}$ $C^{\alpha}H$ peaks were shifted by 0.03 ppm, $Cys_{433}$ was shifted by 0.04 ppm, and $Glu_{426}$ and $Cys_{446}$ were shifted by 0.1 ppm at 15 °C. The $C^{\alpha}H$ shifts of $Asp_{425}$, $Glu_{426}$, $Thr_{443}$, and $Glu_{445}$ are easy to explain since these residues are located within the calcium binding region. The spectral changes of $Cys_{433}$ and $Cys_{446}$ suggest that calcium forces the 2−4 disulfide bond into an appropriate conformation for the cation binding. The calcium effect on $Val_{436}$ resonances was not expected. Both the $C^{\alpha}H$ and NH resonances of $Val_{436}$ were shifted upon the coordination of calcium and may be caused by steric requirements of the peptide−calcium complex formation.

The only unambiguous long-distance NOE connection that markedly increased in intensity upon calcium addition was $His_{438}$ $C^{\beta}H$−$Glu_{445}$ $C^{\gamma}H$. Hence, it is likely that calcium binding favors the formation of the major $\beta$-sheet, which is a conserved structural motif of all EGF-like domains. This assumption is also supported by the behavior of the $C^{\alpha}H$ chemical shifts in the presence and absence of calcium (Figure 7). The downfield shifts of the $C^{\alpha}H$ resonances of the residues 443−447 in the apo form of the [1−3, 2−4] peptide are indicative of the extended backbone conformation of this fragment (*45*). Upon addition of calcium, the $C^{\alpha}H$ resonances of these residues were uniformly shifted even more downfield, thus suggesting an increased tendency of this fragment to adopt an extended conformation.

## DISCUSSION

The fifth and sixth EGF-like domains of TM are believed to be responsible for IIa binding. The recent studies performed by Lougheed et al. (*44*) showed that two peptides derived from the sixth EGF-like domain were much weaker inhibitors of IIa than the peptides from the fifth EGF-like domain. One of these two peptides, cyclic $C_{448}$GPDSALARHIGTD$C_{462}$, represents the C-terminal loop of the sixth domain. The other peptide, cyclic $C_{437}$-HNLPGTFE$C_{446}$, corresponds to the C-terminal loop of the [1−2, 3−4] isomer. Although the minimal TM fragment

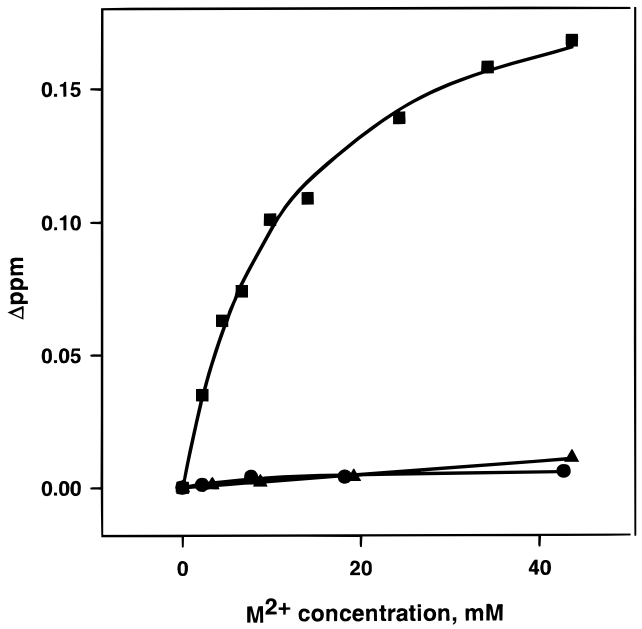


FIGURE 5: Titration of the [1−2, 3−4] and [1−3, 2−4] disulfide-bonded isomers with divalent calcium and magnesium. To the 0.2 mM peptide solutions in 20 mM sodium acetate-$d_3$ buffer, 10% $D_2O$, pH 5.5, small aliquots of $CaCl_2$ or $MgCl_2$ were added in the same buffer at 15 °C. The peptide concentration was maintained constant. The chemical shift changes of the lower field Asn18-$^{\delta}$NH signal in the [1−3, 2−4] (■), [1−2, 3−4] (▲) isomers with respect to $CaCl_2$ concentration and in the [1−3, 2−4] (●) isomer with respect to $MgCl_2$ concentration were monitored.

essential for IIa binding was reduced to the fifth and sixth domains (*46*, *47*), the deletion of the sixth domain from the recombinant human TM decreased its affinity to IIa only 10-fold, whereas the deletion of the fifth domain completely abolished the binding (*47*). Therefore, the weak binding of the above-mentioned peptides derived from the sixth domain brought about questions (*44*) whether the sixth domain directly participates in binding or it just influences the binding of the fifth domain.

We found that the [1−2, 3−4] isomer is indeed a comparatively poor IIa inhibitor, while the crossed [1−3, 2−4] isomer binds IIa more tightly. Apparently, the N-terminal part of the sixth domain directly binds to IIa, thus contributing to the overall binding constant of TM. In addition, since the non-EGF [1−2, 3−4, 5−6] S−S bonding shown in the fifth TM EGF-like domain (*48*, *49*) calls into question the belief that all EGF-like domains have the same disulfide-bonding pattern, our result is an evidence in favor of the "correct" EGF-like cross-linking of the sixth TM EGF-like domain.

The [1−3, 2−4, 5−6] pairing of the sixth EGF-like domain is also supported by the results of the calcium binding studies. The peptide 28EG56 comprising the junction between the fifth and sixth EGF-like modules plus the N-terminal part of the sixth EGF-like module, contains a consensus calcium-binding sequence. However, two different S−S bonded isomers of the peptide respond quite differently to calcium addition. The calcium-induced NMR spectral changes of [1−3, 2−4] bonded isomer of 28EG56 are much more pronounced than that of the [1−2, 3−4] isomer. This result suggests that many residues of the [1−3, 2−4] isomer are directly or indirectly involved in the interaction, thus forming a unique calcium coordination

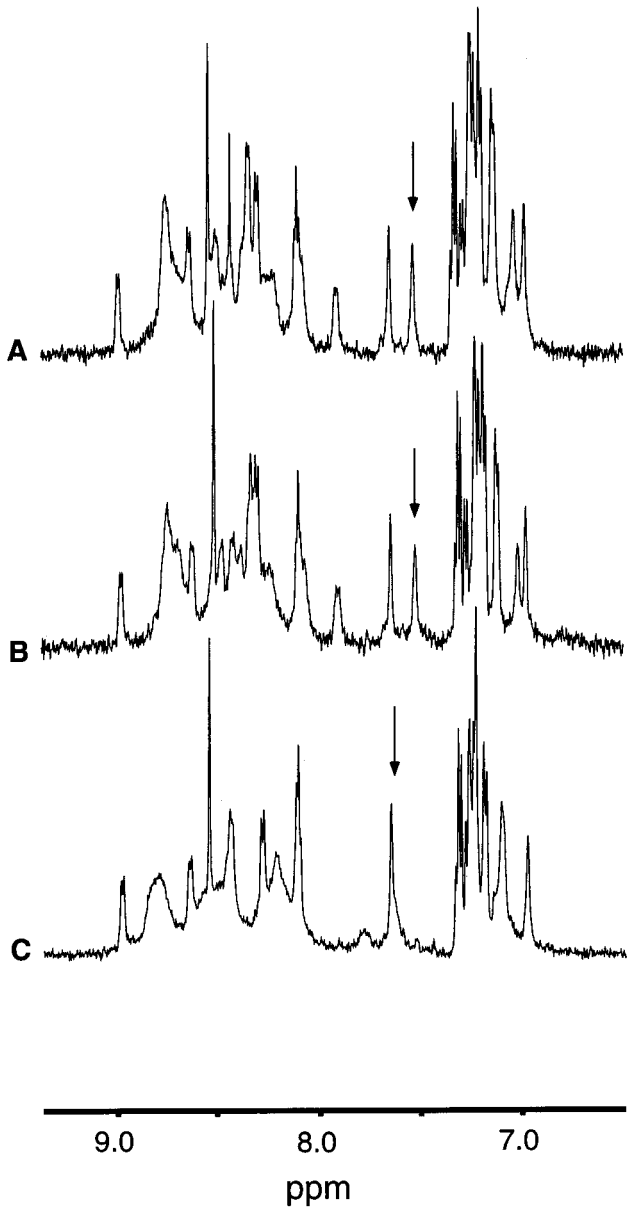


FIGURE 6: The comparative effect of magnesium and calcium on the NMR spectrum of the [1−3, 2−4] isomer. To the solution of *apo*-form (A) of the [1−3, 2−4] isomer, 22 mM of $MgCl_2$ (B) or CaCl2 (C) were added, and NMR spectra were recorded. Only amide proton-to-side-chain regions are displayed. The arrows indicate positions of the low-field Asn18-$^{\delta}$NH resonances for every form. Other experimental conditions were as in Figure 4.

sphere. Calcium binding by the [1−3, 2−4] isomer is rather specific, and very little changes of the NMR spectrum of the peptide were observed in the presence of magnesium.

The ability of the [1−3, 2−4] isomer to bind calcium is an important finding of this work. TM binding to IIa is believed to be calcium independent (*50*, *51*). However, the existence of a calcium-binding site on TM was suggested by the unusual calcium dependence of protein C activation with the active fragment of TM derived from limited proteolysis with elastase (*52*), and by the calcium-dependent fluorescent quenching of this TM fragment (*53*). The role of the TM calcium binding site is not revealed yet, but calcium ion is thought to bridge protein C and TM. The 422−446 region of TM was proposed to bind calcium on the basis of its homology to already known calcium-binding

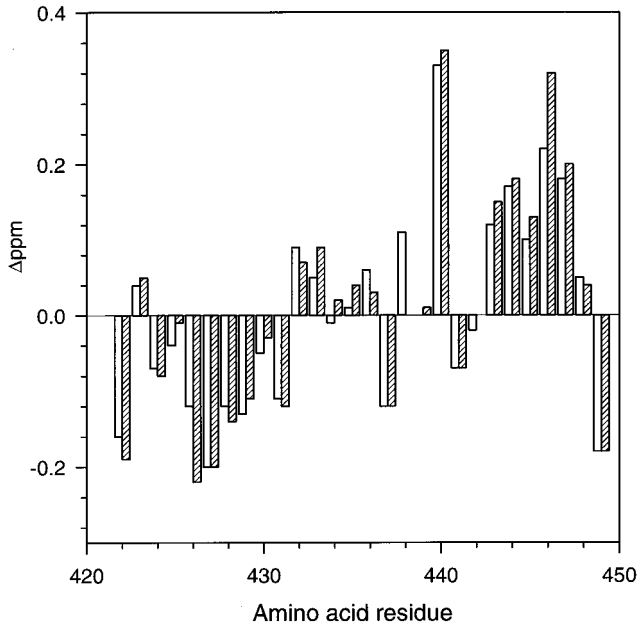


FIGURE 7: Chemical shift index for the $C^{\alpha}H$ proton resonances of the [1−3, 2−4] isomer in apo and calcium-bound form. The values of chemical shift index for apo (open bars) and calcium-bound forms (filled bars) were calculated from data obtained for the [1−3, 2−4] isomer in 20 mM sodium acetate-$d_3$, 10% $D_2O$, pH 5.5, at 15 °C, in the absence and presence of 22 mM $CaCl_2$, through subtraction of the corresponding random coil value (*43*) from the measured value.

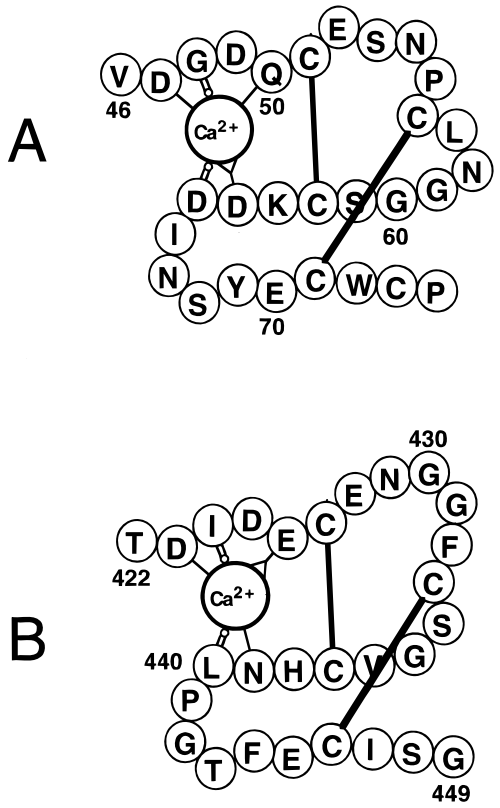


FIGURE 8: The model for the [1−3, 2−4] isomer interaction with calcium. (A) shows the ligands coordinating calcium cation provided by the most closely associated EGF-like domain from human coagulation factor IX as described by Rao et al. (*50*−*54*). (B) represents the predicted ligands for calcium in the corresponding [1−3, 2−4] isomer deduced from NMR resonance perturbations (Figure 4) and analogy with the EGF-like domain from human coagulation factor IX.

EGF-like domains (*25*−*32*) and cofactor activity studies of alanine-substituted mutants of TM (*24*). We present the first direct evidence for the calcium binding of this region.

The calcium-dependent NMR spectral changes of the [1−3, 2−4] isomer are in agreement with the reported X-ray structure of a homologous EGF-like domain from human clotting factor IX in complex with calcium (*54*). In the described EGF-like domain from factor IX the calcium cation interacts with OD1 and OD2 of $Asp_{64}$, OE1 of $Gln_{50}$, OD1 of $Asp_{47}$, and with main-chain carbonyl oxygen atoms of $Gly_{48}$ and $Asp_{65}$ (Figure 8A). In accordance with these results we observed strong chemical shift changes of side-chain protons of $Asp_{423}$, $Glu_{426}$, and $Asn_{439}$ of the [1−3, 2−4] isomer. Apparently, carboxylate/carboxylamide side-chains of these three residues in TM may also supply ligands for complexation with calcium. A model can therefore be proposed for the calcium coordination in the [1−3, 2−4] isomer of the 28EG56 TM fragment (Figure 8B), based on analogy with the EGF-like domain from factor IX (54) and comparison with other consensus calcium-binding EGF-like modules (25, 55).

Side-chain resonances of consensus $Asp_{425}$ were not strongly affected by calcium binding. Apparently, similar to the EGF-like domain from factor IX, this residue does not directly coordinate the cation, but forms a structurally important hydrogen bond with the main-chain amide nitrogen of $Cys_{427}$, which could bring about the observed calcium-induced shifts of the NH and $C^{\alpha}H$ resonances of $Asp_{425}$. Rao et al. (*54*) showed that $Tyr_{69}$ plays an important structural role in factor IX, forming a hydrophobic cluster with $Pro_{55}$. These residues sequentially correspond to $Phe_{444}$ and $Phe_{432}$ of 28EG56. Interestingly, the side-chain resonances of $Phe_{444}$ are strongly affected by calcium binding, while $Phe_{432}$ is tolerant to complex formation. It is possible that calcium binding induces additional hydrophobic interaction involving the side chain of $Phe_{444}$. One of the possible partners for this interaction is $Leu_{440}$, since its side chain resonances exhibit strong changes upon calcium binding as well. Unfortunately, we were not able to observe unambiguous NOE cross-peaks between these two residues to provide additional support for this hypothesis.

To summarize, our data allow us to propose that the structure of the calcium-binding site in the TM consensus calcium-binding fragment is very similar to that of calcium-binding EGF-like domain from factor IX (*54*) (Figure 8). The data presented by Rao et al. (*54*) demonstrated that calcium is coordinated by seven ligands, six of which are supplied by one polypeptide chain and the seventh is supplied by a neighboring EGF-like domain. The seventh coordination site of calcium cation bound to the EGF-like domain can be used for bridging of two proteins, such as TM and protein C. On the other hand, the role of this calcium binding site may be purely structural, and additional experiments are necessary to establish the reason for its presence in the EGF-like domain in TM.

The [1−3, 2−4] isomer is a typical example of the so-called disulfide $\beta$-cross, or the T-knot scaffold, shared by the EGF-like proteins, $\omega$-toxins, plant protease inhibitors (reviewed in refs *33* and *34*), and granulin-like proteins (*56*). The steric requirements for the formation of the central antiparallel $\beta$-sheet reduce the possible disulfide pairings to the criss-cross [1−3, 2−4] cystine pattern (*34*). An example

of the EGF-like domain with a different uncrossed [1−2, 3−4, 5−6] pairing was reported recently (*12*), and the fold did not contain the central $\beta$-sheet characteristic of the T-knot scaffold. The $\beta$-cross with the central antiparallel $\beta$-sheet presents a compact architectural motif that is thought to be a good candidate for a protein folding nucleus (*34*). We observed that free-air oxidation of the peptide comprising the consensus $\beta$-cross sequence, in the presence or absence of redox buffer and/or calcium, produced the uncrossed [1−2, 3−4] pairing. The resulting peptide was a poor IIa inhibitor and had low affinity toward calcium. Forced formation of the crossed [1−3, 2−4] disulfide pairing gave a better IIa inhibitor and better calcium binding. However, even the correct criss-cross disulfide pairing did not produce a well-folded peptide conformation for both apo and calcium-bound forms, as judged by poor amide proton resonance dispersion (approximately 1 ppm) and by very few nonsequential NOE peaks detected. Therefore, the sequence of the EGF6 N-terminal fragment cannot provide enough information for correct folding. Other interactions have to be involved to determine the criss-cross fold in this peptide, most likely the interaction with the C-terminal parts of the fifth and sixth EGF-like domains.

## ACKNOWLEDGMENT

We are grateful to Dr. Ping Xu, Dr. Zhigang Chen, and Anatoly Kutyshenko for technical help with acquiring NMR spectra, and to Betty Zhu for help with NMR data processing and molecular graphics. We thank Dr. J. Song for the critical reading of this manuscript.

## REFERENCES

1. Esmon, C. T. (1989) *J. Biol. Chem. 264*, 4743−4746.
2. Suzuki, K., Stenflo, J., Dahlback, B., and Teodorson, B. (1983) *J. Biol. Chem. 258*, 1914−1920.
3. Fulcher, C. A., Gardiner, J. E., Griffin, J. H., and Zimmerman, T. S. (1984) *Blood 63*, 486-489.
4. Zushi, M., Gomi, K., Yamamoto, S., Maruyama, I., Hayashi, T., and Suzuki, K. (1989) *J. Biol. Chem. 264*, 10351−10353.
5. Parkinson, J. F., Nagashima, M., Kuhn, I., Leonard, J., and Morser, J. (1992) *Biochem. Biophys. Res. Commun. 185*, 567−576.
6. Savage, C. R., Hash, J. H., and Cohen, S. (1973) *J. Biol. Chem. 248*, 7669−7672.
7. Meininger, D. P., Hunter, M. J., and Komives, E. A. (1995) *Protein Sci. 4*, 1683−1695.
8. Hojrup, P., and Magnusson, S. (1987) *Biochem. J. 245*, 887−892.
9. Winkler, M. E., Bringman, T., and Marks, B. J. (1986) *J. Biol. Chem. 261*, 13838−13843.
10. Huang, L. H., Ke, X.-H., Sweeney, W., and Tam, J. P. (1989) *Biochem. Biophys. Res. Communic. 160*, 133−139.
11. Hrabal, R., Komives, E. A., and Ni, F. (1996) *Protein Sci. 5*, 195−203.
12. Benitez, B. A. S., Hunter, M. J., Meininger, D. P., and Komives, E. A. (1997) *Protein Sci. 6*, Suppl. 2, 117.
13. Adler, M., Seto, M. H., Nitecki, D. E., Lin, J. H., Light, D. R., and Morser, J. (1995) *J. Biol. Chem. 270*, 23366−23372.
14. Montelione, G. T., Wuthrich, K., Burgess, A. W., Nice, E. C., Wagner, G., Gibson, K. D., and Scheraga, H. A. (1992) *Biochemistry 31*, 236−249.
15. Hommel, U., Harvey, T. S., Driscoll, P. C., and Campbell, I. D. (1992) *J. Mol. Biol. 227*, 271−282.
16. Baron, M., Norman, D. G., Harvey, T. S., Handford, P. A., Mayhew, M., Tse, A. G. D., Brownlee, G. G., and Campbell, I. D. (1992) *Protein Sci. 1*, 81−90.
17. Graves, B. J., Crowther, R. L., Chandran, C., Rumberger, J. M., Li, S., Huang, K.-S., Presky, D. H., Familletti, P. C., Wolitsky, B. A., and Burns, D. K. (1994) *Nature* (*London*) *367*, 532−538.
18. Hansen, A. P., Petros, A. M., Meadows, R. P., Nettsheim, D. G., Mazar, A. P., Olejniczak, E. T., Xu, R. X., Pederson, T. M., Henkin, J., and Fesik, S. W. (1994) *Biochemistry 33*, 4847−4864.
19. Moy, F. J., Li, Y.-C., Rauenbuehler, P., Winkler, M. E., Scheraga, H. A., and Montelione, G. T. (1993) *Biochemistry 32*, 7334−7353.
20. Nagata, K., Kohda, D., Hatanaka, H., Ichikawa, S., Matsuda, S., Yamamoto, T., Suzuki, A., and Inagaki, F. (1994) *EMBO J. 14*, 3517−3523.
21. Selander-Sunnerhagen, M., Ullner, M., Persson, E., Teleman, O., Stenflo, J., and Drakenberg, T. (1992) *J. Biol. Chem. 267*, 19642−19649.
22. Smith, B. O., Downing, A. K., Driscoll, P. C., Dudgeon, T. J., and Campbell, I. D. (1995) *Structure 3*, 823−833.
23. Padmanabhan, K., Padmanabhan, K. P., Tulinsky, A., Park, C. H., Bode, W., Huber, R., Blankenship, D. T., Cardin, A. D., and Kisiel, W. (1993) *J. Mol. Biol. 232*, 947−966.
24. Nagashima, M., Lundh, E., Leonard, J. C., Morser, J., and Parkinson, J. F. (1993) *J. Biol. Chem. 268*, 2888−2892.
25. Handford, P. A., Mayhew, M., Baron, M., Winship, P. R., Campbell, I. D., and Brownlee, G. G. (1991) *Nature* (London) *351*, 164−167.
26. Huang, L. H., Ke, X. H., Sweeney, W., and Tam, J. P. (1989) *Biochem. Biophys. Res. Commun. 160*, 133−139.
27. Glanville, R. W., Qian, R.-Q., McClure, D. W., and Maslen, C. L. (1994) *J. Biol. Chem. 269*, 26630−26634.
28. Handford, P. A., Downing, A. K., Rao, Z., Hewett, D. R., Sykes, B. C., and Kielty, C. M. (1995) *J. Biol. Chem. 270*, 6751−6756.
29. Knott, V., Downing, A. K., Cardy, C. M., and Handford, P. (1996) *J. Mol. Biol. 255*, 22−27.
30. Dahlback, B., Hildebrand, B., and Linse, S. (1990) *J. Biol. Chem. 265*, 18481−18489.
31. Persson, E., Selander, M., Linse, S., Drakenberg, T., Ohlin, A. K., and Stenflo, J. (1989) *J. Biol. Chem.* 264, 16897−16904.
32. Ohlin, A. K., Linse, S., Stenflo, J. (1988) *J. Biol. Chem. 263*, 7411−7417.
33. Lin, S. L., and Nussinov, R. (1995) *Nat. Struct. Biol. 2*, 835−837.
34. Harrison, P. M., and Sternberg, M. J. E. (1996) *J. Mol. Biol. 264*, 603−623.
35. Kamber, B., Hartmann, A., Eisler, K., Riniker, B., Rink, H., Sieber, P., and Rittel, W. (1980) *Helv. Chim. Acta 63*, 899−915.
36. Gray, W. (1993) *Protein Sci. 2*, 1732−1748.
37. Gray, W. (1993) *Protein Sci. 2*, 1749−1755.
38. Burns, J. A., Butler, J. C., Moran, J., and Whitesides, G. M. (1991) *J. Org. Chem. 56*, 2648−2650.
39. Ni, F., Ripoll, D. R., Martin, P. D., and Edwards, B. F. P. (1992) *Biochemistry 31*, 11551.
40. Ni, F. (1992) *J. Magn. Reson. 99*, 391−397.
41. Braunschweiler, L., and Ernst, R. R. (1983) *J. Magn. Reson. 53*, 521−528.
42. Davis, D. G., and Bax, A. (1985) *J. Am. Chem. Soc. 107*, 2820−2821.
43. Lippens, G., Dhalluin, C., and Wieruszeski, J.-M. (1995) *J. Biomol. NMR 5*, 327−331.
44. Lougheed, J. C., Bowman, C. L., Meininger, D. P., and Komives, E. A. (1995) Protein Sci. *4*, 773−780.
45. Wishart, D. S., Sykes, B. D., and Richards, F. M. (1992) *Biochemistry 31*, 1647−1651.
46. Kurosawa, S., Stearns, D. J., Jackson, K. W., and Esmon, C. T. (1988) *J. Biol. Chem. 263*, 5993−5996.
47. Tsiang, M., Lentz, S. R., and Sadler, J. E. (1992) *J. Biol. Chem. 267*, 6164−6170.
48. Hunter, M. J., and Komives, E. A. (1995) *Protein Sci. 4*, 2129−2134.

49. White, C. E., Hunter, M. J., Meininger, D. P., Garrod, S., and Komives, E. A. (1996) *Proc. Natl. Acad. Sci. U.S.A. 93*, 10177−10182.
50. Esmon, C. T., Esmon, N. L., and Harris, K. W. (1982) *J. Biol. Chem. 257*, 7944−7947.
51. Musci, G., Berliner, L. J., and Esmon, C. T. (1988) *Biochemistry 27*, 769−773.
52. Kurosawa, S., Galvin, J. B., Esmon, N. L., and Esmon, C. T. (1987) *J. Biol. Chem. 262*, 7944−7947.
53. Kurosawa, S., Stearns, D. J., Galvin, J. B., Esmon, N. L., and Esmon, C. T. (1987) *Blood 70*, 389.
54. Rao, Z., Handford, P., Mayhew, M., Knott. V., Brownlee, G. G., and Stuart, D. (1995) *Cell 82*, 131−141.
55. Rees, D. J. G., Jones, I. M., Handford, P. A., Walter, S. J., Esnout, M. P., Smith, K. J., and Brownlee, G. G. (1988) *EMBO J. 7*, 2053−2061.
56. Hrabal, R., Chen, Z., James, S., Bennet, H., and Ni, F. (1996) *Nat. Struct. Biol. 3*, 747−752.

BI9730240